

Galilean satellite ephemerides E5

J.H. Lieske

Jet Propulsion Laboratory, California Institute of Technology,
4800 Oak Grove Dr., MS 301-150
Pasadena, California, USA 91109
E-mail: jay.lieske@jpl.nasa.gov

Received 30.4. 1997; accepted dd.mm.yyyy

Abstract. New ephemerides of Jupiter's **Galilean** satellites are produced from an analysis of CCD astrometric data, Voyager-mission optical navigation images, mutual event observations, photographic plates, and eclipse timing observations. The resulting parameters, for use in the **galsat** computer software, are in the **B1950** frame for use by the Galileo space mission. Results in the **J2000** system are also available.

Key words: astrometry 05.01.1 - celestial mechanics 05.03.1 – ephemerides 05.05.2 – Planets and satellites: Jupiter 07.16.2

1. Introduction

This paper documents the **Galilean** satellite ephemerides designated as E5, which were delivered in support of the Galileo space mission to Jupiter. The E5 ephemerides supersede the E4 ephemerides, which were developed (Lieske 1994a) without using CCD **astrometric** data in order to assess the new data type. It is believed that the E5 ephemerides are better than the E3 and E4 ephemerides and they are recommended for general usage. The parameters of E5 are given in the **B1950** system so that the **galsat** software (Lieske 1977) can be employed directly to compute coordinates in the **B1950** frame, which has been adopted for the Galileo mission.

The ephemerides E2 (Lieske 1980) were developed prior to the Voyager mission and were based solely on an analysis of earth-based observations. The E2 ephemerides utilized mutual event data from 1973 (Aksnes and Franklin, 1976), photographic **astrometric** observations from 1967-1978 (Pascu 1977, 1979), and Jovian satellite eclipse timings from 1878-1974 (Pickering 1907, Pierce 1974, Lieske 1980).

Post-Voyager mission ephemeris improvements yielded ephemerides E3, which included Voyager optical naviga-

tion **astrometric** data and Voyager-derived physical constants (Campbell and Synnott, 1985). The E3 ephemerides employed mutual event data from 1973 and 1979 (Aksnes et al, 1984), Voyager optical navigation **astrometric** measurements from 1979 (Synnott et al 1982), additional **photographic** observations by D. Pascu from 1973-1979, and eclipse timings from 1652 to 1983 (Lieske 1986, 1987).

The initial **pre-Galileo** mission ephemerides were designated E4 (Lieske 1994a) and included extended mutual event data and photographic data, but no CCD observations, since they were still in the process of being evaluated. The E4 ephemerides employed the previously mentioned Voyager data, mutual event data from 1973 and 1979 corrected for phase effects by adding δt to the observation time (Aksnes et al 1986), photographic data and Jovian eclipse timings, as well as additional mutual event **astrometric** measurements from 1985 and 1991 (Aksnes et al 1986; Franklin et al 1991; Kaas et al 1997; Descamps 1994; Goguen et al 1988; Goguen 1994; Mallama 1992), and additional photographic observations from Pascu (1993) covering the interval 1980-1991. Three-years' of CCD data from Flagstaff (Monet et al 1994, Owen 1995) were evaluated, but not employed in developing the **E4** ephemerides.

The E5 ephemerides represent the most current evolution of the **Galilean** satellite ephemerides and incorporate all of the above data types, including an evaluation the Doppler data of Ostro et al (1992).

The 50 parameters which define the theory of motion of the **Galilean** satellites (Lieske 1977) could also be transformed in a manner such that the same **galsat** computer program can be employed to compute rectangular coordinates with their values being in the **J2000** system. Documentation and an algorithm for such transformation of **all galsat-related** ephemerides (e.g., Lieske 1977, 1980; Arlot 1982; Vasundhara 1994) will be issued later. In the meantime the equatorial coordinates can be transformed in the following manner.

For the **Galileo** mission, all input quantities are in the **B1950** frame and Earth equatorial coordinates transformed

mation from B 1950 to J2000 when necessary is done by tile matrix multiplication

$$r_{J2000} = A r_{B1950}, \quad (1)$$

where the matrix A could be taken from that recommended by IAU Commission 20 (West 1992),

$$A = P_{IAU} R_3(-0''.525) \quad (2)$$

with P_{IAU} being the standard IAU precession matrix from B1950 to J2000 (Lieske 1979),

$$P_{IAU} = R_3(-z_A) R_2(\theta_A) R_3(-\zeta_A) \quad (3)$$

or A could be taken from the earlier discussion of Standish (1982), which was developed for transforming from DE118 to DE200,

$$A = R_3(+0''.00073) P_{IAU} R_3(-0''.53160). \quad (4)$$

It essentially consists of a rotation ΔE in the B1950 equatorial plane from the FK4 origin to the dynamical equinox and then processing from B1950 to J2000 using the IAU 1976 equatorial precession parameters P_{IAU} (Lieske et al. 1977).

The matrix A could also be derived from Lieske's discussion (1994b) on the precession of orbital elements,

$$A = R_1(-\epsilon_{J2000}) R_3(L') R_1(-J_A) R_3(-L) R_1(\epsilon_{B1950}). \quad (5)$$

For the Galileo mission, the method of Standish given in Eq. (4) is employed to precess from B1950 to J2000.

The rotation matrices R_i are the standard matrices for rotations about the x , y , or z axes for $i = 1, 2, 3$:

$$\begin{aligned} R_1 &= \begin{bmatrix} 1 & 0 & 0 \\ 0 & \cos \theta & \sin \theta \\ 0 & -\sin \theta & \cos \theta \end{bmatrix} \\ R_2 &= \begin{bmatrix} \cos \theta & 0 & -\sin \theta \\ 0 & 1 & 0 \\ \sin \theta & 0 & \cos \theta \end{bmatrix} \\ R_3 &= \begin{bmatrix} \cos \theta & \sin \theta & 0 \\ -\sin \theta & \cos \theta & 0 \\ 0 & 0 & 1 \end{bmatrix}. \end{aligned} \quad (6)$$

The various matrices mentioned in Eqs (2), (4) and (5) are presented in Table 1. The maximum difference in satellite coordinates, due to the different precessional transformations, is about 1.5 km, so any of the previously mentioned matrices could be used in a practical situation.

2. The basic parameters

In the galsat-type ephemerides, the Jovicentric Earth-equatorial coordinates of the Galilean satellites are computed as a function of 50 "galsat" parameters (Lieske

1977). The definitions of the basic parameters upon which the theory depends are given in Tables 2 and 3. It is seen that they are a combination of physical parameters and orbital elements.

In the E5 ephemerides, we employed the satellite masses ($\epsilon_1 - \epsilon_4$) and Jupiter pole which were determined by Campbell and Synnott (1985) from their analysis of the Voyager data. The Jupiter pole is a function of the longitude of the origin of the coordinates ψ [theory parameter β_{15}], and the inclination I_J of Jupiter's equator to Jupiter's orbit [theory parameter ϵ_{25}], with some dependence upon the Jupiter orbital inclination to the ecliptic [theory parameter ϵ_{26}], Jupiter's node Ω_J [theory parameter β_{22}], and the obliquity ϵ of the ecliptic [theory parameter ϵ_{27}]. The mass of the Jupiter system was that of JPL ephemeris DE 140 (Standish and Folkner 1995) $\text{Sun/Jupiter-system} = 1047.3486$. Ephemerides E3 and E4 employed Jupiter system masses which are consistent with JPL ephemeris DE125 (Standish 1985), $\text{Sun/Jupiter-system} = 1047.349$. The Jupiter pole employed was $\alpha_J = 268^\circ 001$ and $\delta_J = 64^\circ 504$ at the theory epoch JED 2443000.5 and in the B1950 frame. The rate of ψ [theory parameter β_{15}] models the secular motion of Jupiter's pole from the theory epoch. Jupiter's oblateness parameters J_2 and J_4 were also taken from the Campbell and Synnott analysis. They correspond to theory parameters ϵ_{11} and ϵ_{12} in Table 2.

Over the years different tables of AT have been used for the calculation of Ephemeris Time (barycentric dynamical time TDB) minus Universal Time. The appropriate table of AT values depends upon what model of the Moon's tidal acceleration one adopts. The Earth's Moon was most often used to determine values of AT prior to 1955 because of its rapid motion. The derived values of AT effectively depend upon a partitioning into portions due to lunar tidal effects versus real changes in AT. It essentially depends upon the parameter employed to describe the lunar tidal acceleration \dot{n}_{Moon} . The classical determination of $\dot{n}_{Moon} = -22.44 \text{ arcsec/cy}^2$ by Spencer Jones (1939) was employed for the E1 and E2 (Lieske 1980) ephemerides by means of the Brouwer (1952) and Martin (1969) values of AT, which were on the Spencer Jones system.

The Morrison and Ward (1975) value of $\dot{n}_{Moon} = -26.0 \text{ arcsec/cy}^2$ was used for E3, E4 and E5. Tables of AT given by Stephenson and Morrison (1984) can be adjusted for any \dot{n}_{Moon} by the technique noted in Lieske (1987) for times prior to 1955.5 by computing

$$\Delta T(\dot{n}_{Moon}) = \Delta T_{Morrison} - 0.911(\dot{n}_{Moon} + 26)T_0^2 \text{ sec} \quad (7)$$

where T_0 is measured in centuries from the 1955.5 epoch of Morrison (1980). The theory parameters of E1 and E2 are consistent with the Spencer-Jones value of \dot{n}_{Moon} , while those for E3 through E5 are consistent with that of Morrison and Ward.

Table 1. Matrices for precession from B 1950 to J2000

Eq. (2): Commission 20 matrix from $P_{IAU} R_3(-0''.525)$

0.9999256794956877	-0.0111814832204662	-0.0004859003815359
0.0111814832391717	0.9999374848933135	-0.0000271625947142
0.0048590037723143	-0.0000271702937440	0.9999881946023742

Eq. (4): Standish matrix from $R_3(+0''.00073) P_{IAU} R_3(-0''.53160)$

0.9999256791774783	-0.0111815116768724	-0.0048590038154553
0.0111815116959975	0.9999374845751042	-0.0000271625775175
0.0048590037714450	-0.0000271704492210	0.9999881946023742

Eq. (5): Lieake matrix from $R_1(-\epsilon_{J2000}) R_3(L') R_1(-J_A) R_3(-L) R_1(\epsilon_{B1950})$

0.9999256795268940	-0.0111810778339439	-0.0004859930159015
0.0111810775053504	0.9999374894281627	-0.0000272382503387
0.0048599309149990	-0.0000271030297995	0.9999881900987267

Table 2. Definitions of Theory Parameters Epsilon (Theory Table 2)

Epsilon	Parameter	Generating value	Description
1	m_I	$449.7 \cdot 10^{-7}(1 + \epsilon_1)$	Mass of Satellite I relative to Jupiter
2	m_2	$252.9 \cdot 10^{-7}(1 + \epsilon_2)$	Mass of Satellite II relative to Jupiter
3	m_3	$798.8 \cdot 10^{-7}(1 + \epsilon_3)$	Mass of Satellite III relative to Jupiter
4	m_4	$450.4 \cdot 10^{-7}(1 + \epsilon_4)$	Mass of Satellite IV relative to Jupiter
5	S/J	$1047.355(1 + \epsilon_5)$	Mass of Sun relative to Jupiter
6	n_1	$203.48895 \cdot 4208(1 + \epsilon_6)$	Mean motion of Satellite I, <i>deg/day</i>
7	n_2	$101.37472 \cdot 3445(1 + \epsilon_7)$	Mean motion of Satellite II, <i>deg/day</i>
8	n_4	$21.57107 \cdot 1403(1 + \epsilon_8)$	Mean motion of Satellite IV, <i>deg/day</i>
9	λ_A	$180^\circ \epsilon_9 / \pi$	Amplitude of free libration, λ_A in <i>deg</i> , ϵ_9 in <i>rad</i>
10	n_J	$8.3091215712 \cdot 10^{-2}(1 + \epsilon_{10})$	Mean motion of Jupiter, <i>deg/day</i>
11	J_2	$0.01484 \cdot 85(1 + \epsilon_{11})$	Jupiter J_2
12	J_4	$-8.107 \cdot 10^{-4}(1 + \epsilon_{12})$	Jupiter J_4
13	R_J	$71420(1 + \epsilon_{13})$	Radius of Jupiter, <i>km</i>
14	P_J	$9.92482 \cdot 5(1 + \epsilon_{14})$	Period of Jupiter rotation, <i>hr</i>
15	$3(C - A)/2C$	$0.111(1 + \epsilon_{15})$	Ratio of Jupiter moments of inertia
16	e_{11}	$465 \cdot 10^{-7}(1 + \epsilon_{16})$	Primary eccentricity of Satellite I, <i>rad</i>
17	e_{22}	$825 \cdot 10^{-7}(1 + \epsilon_{17})$	Primary eccentricity of Satellite H, <i>rad</i>
18	e_{33}	$15164 \cdot 10^{-7}(1 + \epsilon_{18})$	Primary eccentricity of Satellite III, <i>rad</i>
19	e_{44}	$73725 \cdot 10^{-7}(1 + \epsilon_{19})$	Primary eccentricity of Satellite IV, <i>rad</i>
20	e_J	$0.0484602472(1 + \epsilon_{20})$	Eccentricity of Jupiter
21	c_{11}	$4756 \cdot 10^{-7}(1 + \epsilon_{21})$	Primary sine inclination of Satellite I
22	c_{22}	$81490 \cdot 10^{-7}(1 + \epsilon_{22})$	Primary sine inclination of Satellite H
23	c_{33}	$31108 \cdot 10^{-7}(1 + \epsilon_{23})$	Primary sine inclination of Satellite III
24	c_{44}	$47460 \cdot 10^{-7}(1 + \epsilon_{24})$	Primary sine inclination of Satellite IV
25	I_J	$3.10401(1 + \epsilon_{25})$	Inclination of Jupiter orbit to Jupiter equator, <i>deg</i>
26	J	$1.30691(1 + \epsilon_{26})$	Inclination of Jupiter orbit to ecliptic, <i>deg</i>
27	ϵ	$23^\circ 26' 44''.84(1 + \epsilon_{27})$	Inclination (Obliquity) of ecliptic to Earth equator <i>deg</i>
28	n_S	$3.3459733896 \cdot 10^{-2}(1 + \epsilon_{28})$	Mean motion of Saturn, <i>deg/day</i>

Table 3. Definitions of Theory Parameters Beta (*Theory* Table 3)

Beta	Parameter	Epoch value (deg)	Description
1	e_1	106°? 03042 +01	Mean longitude of Satellite I
2	ℓ_2	175°74748 + β_2	Mean longitude of Satellite II
3	ℓ_3	[120°? 60601 - $\frac{1}{2}\beta_1 + \frac{3}{2}\beta_2$]	Mean longitude of Satellite III
4	ℓ_4	84851861 + β_4	Mean longitude of Satellite IV
5	ϕ_λ	β_5	Free Libration $\psi_1 - 3\psi_2 + 2\psi_3 = \pi + \epsilon_9 \sin \phi_\lambda$ $= 180^\circ + \lambda_A \sin \phi_\lambda$
6	π_1	4°51172 + β_6	Proper periapse of Satellite I
7	π_2	74°53051 + β_7	Proper periapse of Satellite II
8	π_3	174°85831 + β_8	Proper periapse of Satellite III
9	π_4	336°02667 + β_9	Proper periapse of Satellite IV
10	Π_J	13°30364 + β_{10}	Longitude of perihelion of Jupiter
11	ω_1	242°73706 + β_{11}	Proper node of Satellite I
12	ω_2	95°28556 + β_{12}	Proper node of Satellite II
13	ω_3	125°14673 + β_{13}	Proper node of Satellite III
14	ω_4	317°89250 + β_{14}	Proper node of Satellite IV
15	ψ	316°73369 + β_{15}	Longitude of origin of coordinates (Jupiter's pole)
16	G'	31°97852 80244 + β_{16}	Mean anomaly of Saturn
17	G	30°37841 20168 + $\beta_{17} + \delta G$	Mean anomaly of Jupiter
18	ϕ_1	172°84(1 - 0.014ϵ_{20}) + β_{18}	Phase angle in solar $(A/R)^3$ with angle $2G' - G$
19	ϕ_2	47°03(1 - 0.156ϵ_{20}) + β_{19}	Phase angle in solar $(A/R)^3$ with angle $5G' - 2G$
20	ϕ_3	259°18 + β_{20}	Phase angle in solar $(A/R)^3$ with angle $G' - G$
21	ϕ_4	157°12(1 + 0.0014ϵ_{20}) + β_{21}	Phase angle in solar $(A/R)^3$ with angle $2G' - 2G$
22	Ω_J	99°95326 + β_{22}	Longitude ascending node of Jupiter's orbit on ecliptic

Beta	Symbol	Rate (deg/day)	Description
1	$\dot{\ell}_1$	203°48895 4208(1+ ϵ_6)	Mean motion of Satellite I
2	$\dot{\ell}_2$	101 S37472 3445(1+ ϵ_7)	Mean motion of Satellite II
3	$\dot{\ell}_3$	[50°3176080635{1 - 2ϵ_6 + 3ϵ_7 -0.02204 51849 7($\epsilon_6 - \epsilon_7$)}}]	Mean motion of Satellite III
4	$\dot{\ell}_4$	21°57107 1403(1+ ϵ_8)	Mean motion of Satellite IV
5	$\dot{\phi}_\lambda$	a(=0°17379190 + . ..)	Rate of free libration (Fiche Table A.30)
6	$\dot{\pi}_1$	(0°1613 8586+ ...)	Proper periapse rate of Satellite I
7	$\dot{\pi}_2$	(0°0472 6307 +...)	Proper periapse rate of Satellite II
8	$\dot{\pi}_3$	(0°0071 2734 +...)	Proper periapse rate of Satellite III
9	$\dot{\pi}_4$	(0°0018 WOO+ ...)	Proper periapse rate of Satellite IV
10	$\dot{\Pi}_J$	0	
11	$\dot{\omega}_1$	(-0°1327 9386 +...)	Proper node rate of Satellite I
12	$\dot{\omega}_2$	(-0°0326 3064+ . .)	Proper node rate of Satellite II
13	$\dot{\omega}_3$	(-0°0071 7703 +...)	Proper node rate of Satellite III
14	$\dot{\omega}_4$	(-0°0017 5934+ ...)	Proper node rate of Satellite IV
15	$\dot{\psi}$	(-0°0000 0208+ ...)	Longitude of origin rate
16	\dot{G}'	3°3459733896 $\cdot 10^{-2}(1 + \epsilon_{28})$	Mean motion of Saturn
17	\dot{G}	8°30912 15712. $\cdot 10^{-2}(1 + \epsilon_{10})$	Mean motion of Jupiter
18...22		0	

3. The observations

A variety of different observational data types were employed in developing ephemerides E5. A new and very powerful data type of CCD observations from the U.S. Naval Observatory Flagstaff Station was used for the first time, together with very accurate Voyager optical navigation data from 1979 and the mutual event observations 1973-1991, photographic observations of D. Pascu from 1967-1993 and Jovian eclipse timings from 1652-1983. Doppler observations from 1987-1991 were employed to assess the value of the Doppler data and evaluate the ephemerides. By intercomparing various data types one learns of the strengths and weaknesses of each individual type of data and discovers inconsistencies among the data types. The data are described in Table 4, which also gives the percentage change in weighted sum-of-squares for ephemeris E5 relative to ephemeris E3. A plus sign indicates an increase and a minus sign indicates a decrease in the weighted residuals. The various data types were combined by weighting each observation by the reciprocal of its squared apriori standard deviation,

Table 4. Observational data employed for ephemeris E5

Data span	observable type	observ.	% chg
1992-1994	CCD data, Flagstaff ra & dec	870	-52.6
1979	Voyager opnav ra & dec	366	-19.0
1973-1991	mutual events ra & dec	860	-55.5
1967-1993	photographic ra & dec	8462	-3.2
1652-1983	eclipse timings	15711	+2.7
1994	CCD data, Table Mountain	72	+68.3
1987-1991	Doppler	50	-55.6

3.1. CCD observations

The new CCD observations were made at the U.S. Naval Observatory Flagstaff Station (A. Monet *et al* 1994) during the years 1993-1995, employing techniques developed by D. Monet and described in Monet *et al* (1992) and in Monet and Monet (1992). The Flagstaff data were processed at JPL by W. Owen who produced normal-point residuals, typically from 30-50 CCD “exposures”, for the author using ephemeris E3. Those residuals were then employed by the author to generate pseudo-observable “normal-point observations” by adding the residual to an artificially-constructed computed position at the mean time of the CCD exposures using the same ephemeris which was employed in computing the CCD residuals. Such a “normal point observation” could be employed with other astrometric data in an analysis of the observations, and should represent a valid description of the actual CCD observations. Additionally, the pseudo-

observations will serve the purpose of archiving the CCD observations in convenient form. In processing the CCD data Owen would estimate the pointing and orientation parameters and employ a single telescope scale factor (modified for refraction and atmospheric effects) for all the Flagstaff data and he would use a single ephemeris (viz, E3) which was not adjusted in the reduction process. If that procedure is valid, then the pseudo-observables generated should behave like valid observational data, viz. the residuals should decrease if one employs a better ephemeris with the original pseudo-observables. It was for this reason that ephemeris E3 was intentionally employed – it was known to need some correction and we desired to explore the validity of the process of constructing normal point pseudo-observables. If the normal points were constructed instead on a different ephemeris, then the pseudo-observables differed by less than 15 km (0''005) from those generated via ephemeris E3, even though the residuals might actually be significantly different using the two ephemerides. That 15-km reproducibility of the normal points is a good indication of the intrinsic accuracy of the CCD data.

Some less-accurate CCD data from the JPL Table Mountain Facility (Owen 1995) were also employed, although with hindsight they probably should not have been included in developing E5. They did not exhibit the reduction of residuals with a better ephemeris, and that is believed to be due to the fact that there were too few Table Mountain data to adequately separate the orbital effects from the telescope effects.

The CCD data were processed using Lambert scattering to compute the offset between the center of light and center of figure (Lindgren 1977) and it is believed that the dominant remaining unmodeled error source in these data is due to albedo variations across the disk of the satellites. Recent estimates of the albedo variations by several scientists (Goguen 1994, Mallama 1993, Riedel 1994, Gaskell 1995) are not entirely consistent and for the Galileo-mission ephemerides it was decided to limit the processing to computation of the difference between center of light and center of figure due to Lambert scattering only, since it represents a reasonable first approximation to the scattering properties of the satellites if one excludes albedo variations (viz., effects which depend upon features on the satellites and which vary with planetocentric longitude of the central disc). The extrapolation of Voyager-derived scattering properties (which occurred at high phase angle) to the scattering properties of the satellites at low phase angle as observed from the Earth is not entirely satisfactory and the several efforts done to date are not entirely consistent with one another. It is hoped that some series of observations made from the Hubble Space Telescope will resolve the problems.

The Flagstaff CCD data were weighted using a standard deviation of 0''.03, which corresponds to about 90 km for these earth-based observations. The Table Mountain

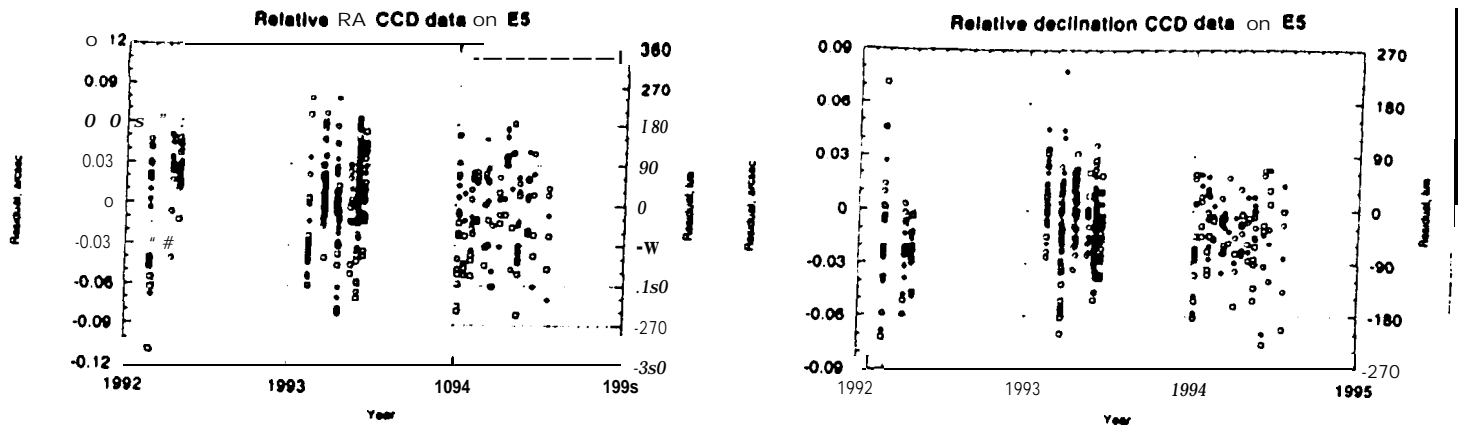


Fig. 1. Residuals in right ascension (left) and declination (right) for Flagstaff CCD observations relative to Satellite 1 using ephemeris E5. The observations of Europa relative to $_{10}$ are indicated by a \circ , those of Ganymede by a \square , and those of Callisto by a \triangle .

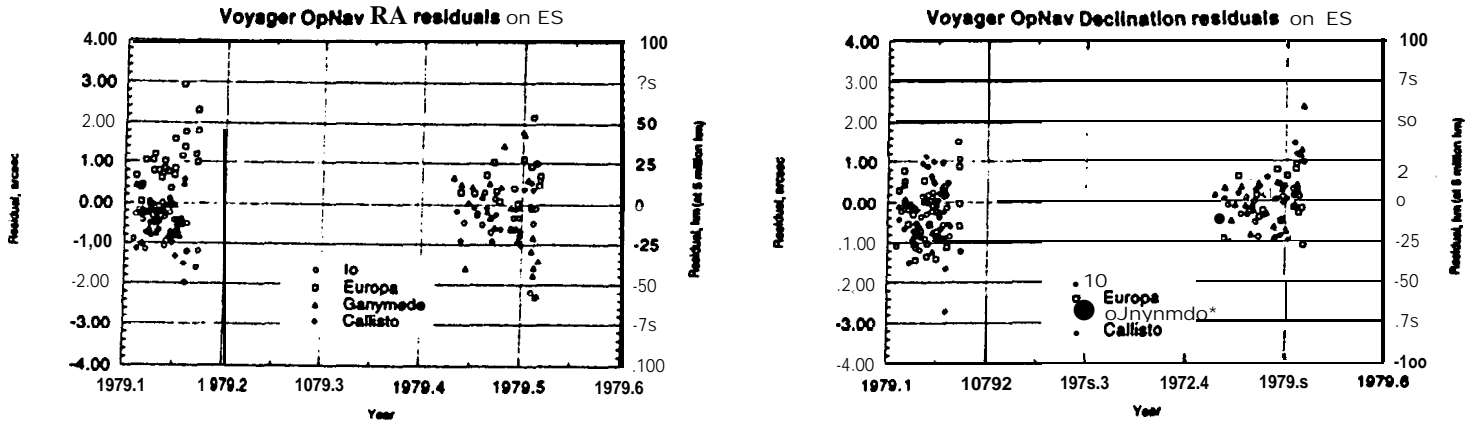


Fig. 2. Residuals in right ascension (left) and declination (right) for the Voyager optical navigation observations using ephemeris E5. The ordinate is in arcsec with an approximate corresponding linear distance scale on the right. Jupiter-relative observations of Io are indicated by \circ , Europa by \square , Ganymede by \triangle , and Callisto by \diamond .

data were weighted using a standard deviation of $0''.05$, corresponding to about 150 km.

3.2. Voyager optical navigation data

During the Voyager mission in 1979, some optical navigation images of the Jovian satellites were taken from the spacecraft for use in navigating the spacecraft to the Jovian encounter. We have 183 observations of the Jovian satellites in right ascension and in declination, made during the Voyager I and Voyager 11 encounters (Synnott et al, 1982). The optical navigation images are analogous to earth-based astrometric observations of the satellites except that the "opnav" images are taken by an "observer" much closer to the Jovian system (typically 13–95 light seconds from the satellites). At $5 \cdot 10^6$ km from Jupiter, one arcsec corresponds approximately to 25 km. Additionally,

the spacecraft-based observations are the result of analyzing extended satellite images. By inferring the center of the satellite from observations of the limb, the Voyager data do not have the center-of-light vs center-of-figure problems which are common to disk-integrated images such as those contained in CCD observations and photographic plates and mutual events. The Voyager data were weighted using a standard deviation of $1''.0$. For spacecraft-to-satellite distances of 13–95 light seconds, the $1''.0$ corresponds to 19 and 140 km respectively for these spacecraft-based observations. The Voyager optical navigation residuals on ephemeris ES are depicted for right ascension and declination in Fig. 2.

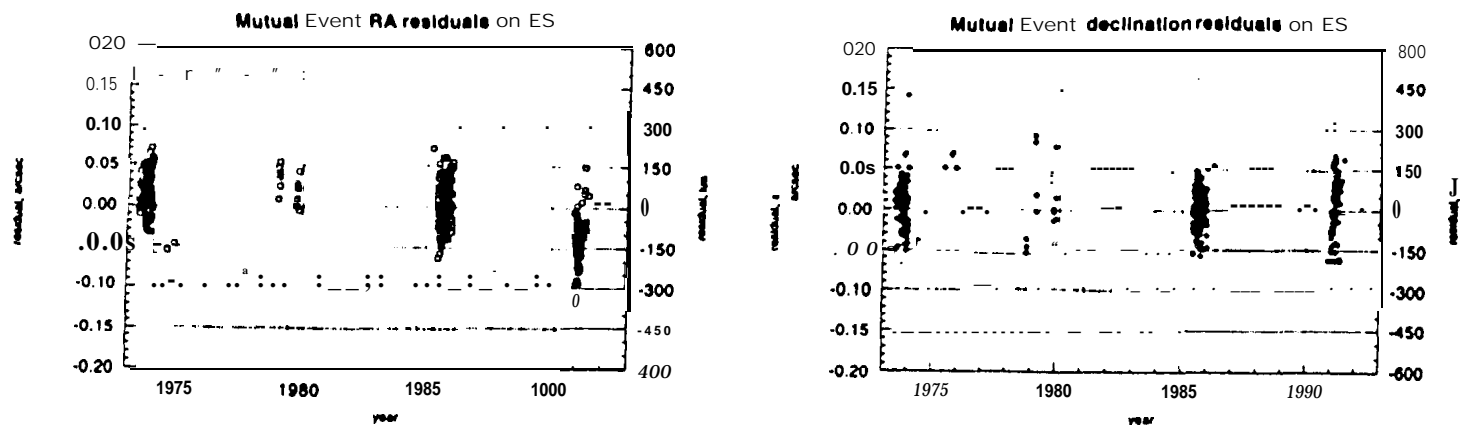


Fig. 3. Residuals in right ascension (left) and declination (right) for astrometric mutual event observations using ephemeris ES. The ordinate is in arcsec with an approximate corresponding linear distance scale on the right.

3.3. Mutual event astrometric data

Since 1973 there have been successful campaigns to observe the mutual event seasons every six years, when the Jovian satellites eclipse and occult one another as the Sun and the Earth pass through the plane of the Jovian equator, in which the satellite orbits lie, Aksnes and colleagues (Aksnes 1974, 1984; Aksnes and Franklin 1978, 1990), along with Arlot and colleagues (Arlot 1978, 1984, 1990, 1996), have made predictions of such mutual events available to scientists throughout the world and have organized scientific programs to observe the mutual events. Aksnes' team has produced astrometric separations of the satellites, at times near the mid-event times, which are very useful for ephemeris development purposes.

The early Galilean satellite ephemerides E1 and E2 (Lieske 1980) employed the Aksnes data from 1973 (Aksnes and Franklin 1976) and 1979 (Aksnes et al 1984) and were affected by the phase offsets between eclipses and occultations which led Aksnes et al (1986) to recommend that δt be added to the published observation times for the 1973 and 1979 data. The ephemerides E3 were generated using the recommended additions of δt to the observation times in processing the 1973 and 1979 mutual events astrometric data.

In the processing of mutual event observations by the Aksnes team in 1985 (Franklin et al 1991) and 1991 (Kaas et al 1997), it was intended that no value of δt would be required but that instead the authors would incorporate the phase effects into their published times and separations. However, the effects were added in the incorrect direction for the published data and hence it is recommended (Aksnes 1993, Franklin 1993, Lieske 1995) that the 1985 and 1991 Aksnes data be employed by adding *twice* the published values of the δt phase corrections to the observation times. Essentially the first addition of δt removes the erroneous application of the phase effects with the incorrect

sign and the second application of δt actually corrects for the phase problem. Additionally, some infra-red astrometric mutual event separations were obtained from Goguen et al (1988) in 1985 as well as in 1991 (Goguen 1994). Astrometric separations from the 1991 mutual event season which were employed in the development of ES were also published by Mallama (1992a), Spencer (1993) and by Descamps (1994).

The mutual event data were weighted using standard deviations of $0''.020$ to $0''.045$, which corresponds to 60 km and 140 km respectively for these earth-based observations. The typical weight corresponds to a standard deviation of $0''.030$ or 90 km.

The obvious offset in right ascension residuals for the 1991 mutual event season depicted in Fig. 3 is believed not to be due to ephemeris errors, but rather is due to albedo effects since almost all of the 1991 mutual event observations involved Io and were made at comparable longitudes on the satellite disk. The CCD and photographic data, for example, show no such offset and those data were sampled at various longitudes.

3.4. Photographic observations

The long and valuable series of photographic observations made by D. Pascu of the U.S. Naval Observatory have been an essential ingredient of the Galilean satellite ephemerides since the first development of the Galsat software. In an extended series of observations 1967-1993, Pascu (1977, 1979, 1993, 1994) provided astrometric observations of the satellites. He pioneered the development of neutral density filters to enable the accurate observation of the Galilean satellites on a regular basis. The Pascu data were reduced using a single scale factor (modified by adjustments for refraction for each observation) for the ensemble of observations, as determined by Pascu. Additionally, a correction to the Pascu scale was applied for a

refraction-related effect, amounting to a relative change in scale of $-5 \text{ S}''/206265$, which probably resulted from the manner in which the plate scale was originally determined.

The photographic data from 1967 through 1975 were weighted using a standard deviation of $0''.13$ per exposure, while those from 1976 onwards were weighted using a standard deviation of $0''.09$ per exposure, corresponding to position uncertainties of 400 km and 275 km, respectively, for each exposure. A photographic plate typically consisted of 4 exposures of each satellite.

The residuals on E5 for photographic observations are plotted in Fig. 4. In the figure, normal-point residuals are presented for each photographic plate, in order to make the comparison with the normal-point CCD observations more feasible. In the plots, the residuals for all exposures of a given satellite on a single plate are averaged into a single normal-point residual.

3.5. Jupiter eclipse timings

The Jovian eclipse timings, representing the classical observations of the Galilean satellites back to the 17th century, were discussed in Lieske (1986a, b). The early data are from the Pingré 17th century collection later published by Bigourdan (1901), and from the Delisle collection (Bigourdan 1897). The book on 17th century astronomy by Pingré published by Bigourdan was originally scheduled for publication 100 years earlier by Pingré. But Pingré's death and the French revolution intervened, and the printer's proof copies were destroyed as scrap paper. It was only 100 years later that a copy of the proofs was found and ultimately published by the Paris Academy. The manuscript collection of J.-N. Delisle contains a wealth of historically and scientifically interesting observations of Galilean satellite eclipses. These two collections effectively re-construct the "lost" Delambre collection.

We employed satellite radii of 1815, 1569, 2631 and 2400 km for Io through Callisto, respectively (Davies et al 1985), in reducing the eclipse timings.

Additionally, the series of eclipse observations by Pickering from 1878-1903 (Pickering 1907) and those accumulated by Pierce (1974), together with those of many amateur astronomers, especially those coordinated by B. Loader and J. Westfall, were employed. Finally, a few eclipse timings by Mallama (1992b) taken in 1990-91 were analyzed.

The eclipse timing data were employed with average standard deviations between 44 sec for Io and 150 sec for Callisto with a mean of 63 sec, which correspond to position uncertainties of 775 km for Io, 1225 km for Callisto, and 800 km on the average for all satellites. The residuals appear visually similar to those depicted in Lieske (1986a) and therefore they are not presented here again.

3.6. Doppler data

The Doppler observations discussed by Ostro et al (1992) were employed to evaluate the ephemerides and explore the potential of Doppler data, but they were not included in analysis and the development of E5. The data are consistent with the observations which were analyzed, but they were not included in the analysis because of possible uncertainty in the radar scattering properties of the satellites similar to albedo effects which depend upon the planetocentric longitude. The 50 Doppler observations of the outer three Galilean satellites were made between 1987 and 1991.

The Doppler data were weighted using standard deviations of 19 Hz for Europa, 12 Hz for Ganymede and 10 Hz for Callisto for the Arecibo 13-cm S-band system data.

4. Discussion

The theory parameters which result from the analysis of these data are listed in Table 5, which will produce coordinates in the B1950 frame when used with the galsat software. A future paper will document how they, and any other set of galsat parameters, can be transformed to the J2000 system in a manner such that the galsat software will directly produce J2000 coordinates. In Table 5, the uncertainties listed for the ϵ and β parameters are the formal errors obtained in the estimation process. By comparing the coordinates of ephemerides E3 with those of E5 and interpreting those differences to represent a $1-\sigma$ error, we obtain a scale factor which should be applied for the formal uncertainties listed in the table. That scale factor ranges between 2.5 and 3, so we recommend that the formal errors be multiplied by 3. The derived values of the angular variables for E5 are given in Table 6. The series coefficients for satellite coordinates ξ , v and ζ are summarized in Table 7 for the E5 ephemerides.

Representing the Jupiter-equatorial projection of the orbital radius by ρ , and the true and mean longitudes by ν and ℓ , respectively, then the equatorial radial component $\xi = (\rho - a)/a$ consists of cosine terms $\xi(t) = \sum K_1 \cos \Theta_1(t)$, while the longitude component $v = \nu - \ell$ consists of sine terms $v(t) = \sum K_2 \sin \Theta_2(t)$, and the latitude component $\zeta = \bar{z}/a$ consists of sine terms $\zeta(\tau) = \sum K_3 \sin \Theta_3(\tau)$. As developed by Sampson (1921, pp. 229-230), the "time-completed" τ may be defined as

$$\tau = t + v/n, \quad (8)$$

where t is "ephemeris time" (TDB). One can employ the time-completed to compute the latitude quantity $s(t) = \bar{z}/\rho$ from the shorter series for $\zeta(t) = .2/a$ via the relationship $s(t) = \zeta(t + v/n)$. It effectively amounts to calculating the latitude perturbations as a function of true longitude rather than as a function of mean longitude.

The Jupiter equatorial coordinates $\bar{\mathbf{r}} = (\bar{x}, \bar{y}, \bar{z})^T$ are computed from the orbital components ξ , u , ζ using the

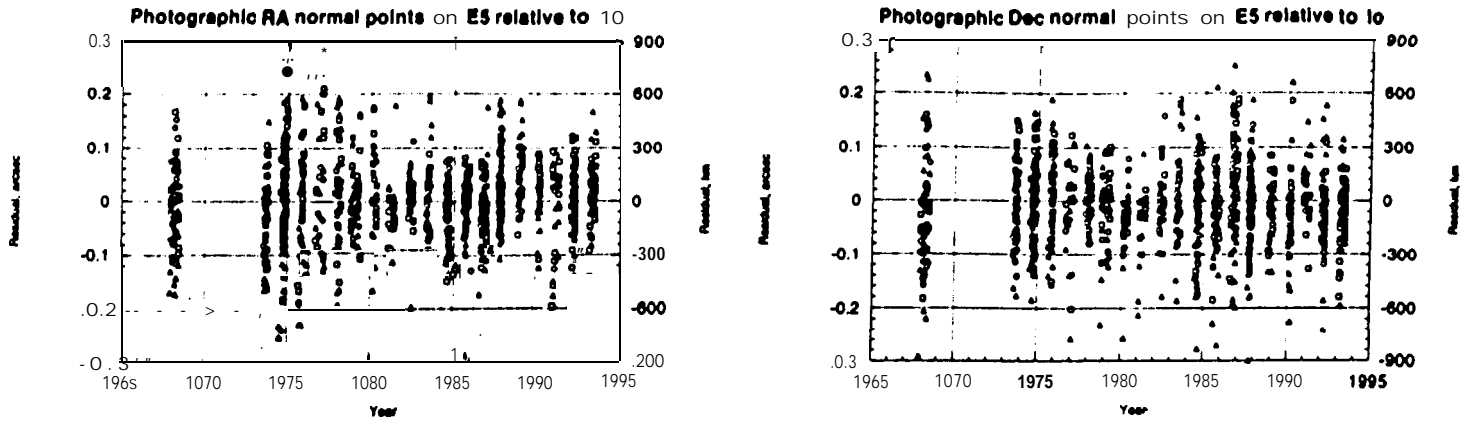


Fig. 4. Residuals in right ascension (left) and declination (right) for photographic observations relative to Io using ephemeris E5. The residuals for exposures of a given satellite on each plate have been combined to produce a normal point for each plate. observations of Europa relative to Io are indicated by \circ , those of Ganymede by \square and those of Callisto by \triangle .

Table 5. Values of theory parameters ϵ and β for Es in B1950 frame [see also Tables 2 and 3].

Parameter	related to	Value	Parameter	Related to	Value
ϵ_1	m_1	0.046323 (± 0.000813)	ϵ_{26}	J	-0.000137 (± 0.000117)
ϵ_2	m_2	-0.000906 (± 0.001394)	ϵ_{27}	ϵ	0.000000 (± 0.000004)
ϵ_3	m_3	-0.022997 (± 0.000276)	ϵ_{28}	n_S	0.000000 (± 0.000001)
ϵ_4	m_4	0.258508 (± 0.000537)	β_1	ℓ_1	0°046767 (± 0.00218)
ϵ_5	S/J	2009.3457E -07 ($\pm 8.12E - 07$)	β_2	ℓ_2	-0°015865 (± 0.000835)
ϵ_6	n_1	7.7760E -09 ($\pm 0.549E - 09$)	β_3	ℓ_3	$[\ell = -\frac{1}{2}\beta_1 + \frac{3}{2}\beta_2]$
ϵ_7	n_2	12.7230E -09 ($\pm 1.04E - 09$)	β_4	ℓ_4	-0°074023 (± 0.001950)
ϵ_8	n_4	-10.4916E -09 ($\pm 4.90E - 09$)	β_5	ϕ_λ	199°2676608 (± 1.57)
ϵ_9	λ_A	11.2104E -04 ($\pm 0.391E - 04$) rad	β_6	π_1	92°576366 (± 19.9)
ϵ_{10}	n_J	1.63E -05 ($\pm 0.13E - 05$)	β_7	π_2	80°335825 (± 1.35)
ϵ_{11}	J_2	-0.007576 (± 0.000066)	β_8	π_3	13°325727 (± 0.150)
ϵ_{12}	J_4	-0.275934 (± 0.00631)	β_9	π_4	-0°739863 (± 0.0152)
ϵ_{13}	R_J	-0.000306 (± 0.000057)	β_{10}	Π_J	0°166302 (± 0.00344)
ϵ_{14}	P_J	9.5E -06 ($\pm 102.E - 06$)	β_{11}	ω_1	69°597506 (± 0.768000)
ϵ_{15}	$3(C - A)/2C$	-0.170000 (± 0.0676)	β_{12}	ω_2	5°155556 (± 0.0495)
ϵ_{16}	e_{11}	-0.995346 (± 0.0291)	β_{13}	ω_3	-5°952489 (± 0.101)
ϵ_{17}	e_{22}	0.748031 (± 0.0221)	β_{14}	ω_4	4°726133 (± 0.0772)
ϵ_{18}	e_{33}	-0.051182 (± 0.00167)	β_{15}	ψ	-0°215487 (± 0.00545)
ϵ_{19}	e_{44}	-0.002434 (± 0.000324)	β_{16}	G'	0°000000 (± 0.407)
ϵ_{20}	e_J	0.002750 (± 0.000081)	β_{17}	G	-0°140855 (± 0.00279)
ϵ_{21}	c_{11}	0.344275 (± 0.0196)	β_{18}	ϕ_1	15°541000 (± 0.411)
ϵ_{22}	c_{22}	-0.005970 (± 0.000872)	β_{19}	ϕ_2	5°215000 (± 0.469)
ϵ_{23}	c_{33}	0.041611 (± 0.00199)	β_{20}	ϕ_3	-1°996000 (± 0.757)
ϵ_{24}	c_{44}	-0.070074 (± 0.000810)	β_{21}	ϕ_4	-7°963000 (± 0.293)
ϵ_{25}	I_J	0.005110 (± 0.000079)	β_{22}	Ω_J	0°045266 ($\pm 0.0066-1$)

Table 6. Derived variables for ephemeris E5

Index	Variable	Value (deg)	Rate (deg/day)
1	ℓ_1	106°? 077187	203°48895579033
2	ℓ_2	175°? 731615	101°?37472473479
3	ℓ_3	120°? 558829	50°31760920702
4	ℓ_4	84°444587	21°57107117668
5	ϕ_λ	199.676608	0°?17379190461
6	π_1	97°088086	0°16138586144
7	π_2	154°866335	0°04726306609
8	π_3	188°184037	0°00712733949
9	π_4	335°286807	0°00183999637
10	Π_J	13°469942	0.
11	ω_1	312°334566	-0°?13279385940
12	ω_2	100°441116	-0°03263063731
13	ω_3	119°194241	-0°00717703155
14	ω_4	322°618633	-0°00175933880
15	ψ	316°518203	-2°?08362. 10-6
16	G'	31°978528	0°03345973390
17	G	30°237557	0°?08309257010
18	ϕ_1	188°374346	0.
19	ϕ_2	52°224824	0.
20	ϕ_3	257°184000	0.
21	ϕ_4	149°152605	0.
22	Ω_J	99°998526	0.
	a_1		2.819353 .10-3 au.
	a_2		4.485883 .10-3 a.u.
	a_3		7.155366 .10-3 a.u.
	a_4		12.585464 .10-3 au.

equations

$$\begin{aligned}\bar{x} &= a(1 + \xi) \cos(\ell - \psi + v) \\ \bar{y} &= a(1 + \xi) \sin(\ell - \psi + v) \\ \bar{r} &= a(1 + \xi)s.\end{aligned}\quad (9)$$

The Earth-equatorial coordinates $\mathbf{r} = (x, y, z)^T$ are then computed from the Jupiter-equatorial coordinates via the rotation matrices

$$\mathbf{r} = R_1(-\varepsilon)R_3(-\Omega)R_1(-J)R_3(-\psi + \Omega)R_1(-I)\bar{\mathbf{r}}. \quad (10)$$

It is these Earth-equatorial coordinates \mathbf{r} that are provided by the galsat software.

As described in *Theory*, the Earth-equatorial coordinates are constructed from the series for ξ, v and ζ by the relationship

$$\begin{aligned}\xi(t) &= \Sigma K_1 \cos \Theta_1(t) \\ v(t) &= \Sigma K_2 \sin \Theta_2(t) \\ s(t) = \zeta(\tau) &= \Sigma K_3 \sin \Theta_3(\tau)\end{aligned}\quad (11)$$

where the right-hand sides are the result of computing the series given in Table 7. The third equation for $s(t)$ employs the time-completed $\tau = t + u/n$ to evaluate the series for $\zeta(\tau)$ and thus to obtain $s(t)$.

The adjustable parameters ε and β for ephemerides E5 in the B1950 frame are given in Table 5. The derived values of the angular variables for E5 are given in Table 6.

Acknowledgements. This paper represents the results of one phase of research conducted at the Jet Propulsion Laboratory, California Institute of Technology, under contract with the National Aeronautics and Space Administration. The CCD observations were made by D. and A. Monet of the USNO Flagstaff Station and were processed into right-ascension and declination normal-point residuals on a fixed ephemeris by W.M. Owen Jr at JPL.

References

- Aksnes, K. 1974, *Icarus* 21, 100
Aksnes, K., Franklin, F., 1976, *AJ* 81, 464
Aksnes, K., Franklin, F., 1978, *Icarus* 34, 188
Aksnes, K. 1984, *Icarus* 60, 180
Aksnes, K., Franklin, F., Millie, R., Birch, B., Blanco, C., Catalane, S., Piironen, J., 1984, *AJ* 89, 28; *AJ* 89)1081
Aksnes, K., Franklin, F., Magnusson, P., 1986, *AJ* 92, 1436
Aksnes, K., Franklin, F., 1990, *Icarus* 84, 542
Aksnes, K., 1993, Personal communication
Arlot, J.-E., 1978, *A&A Supp* 34, 195
Arlot, J.-E., 1982, *A&A* 107, 305
Arlot, J.-E., 1984, *A&A* 138, 113
Arlot, J.-E., 1990, *A&A* 237, 259
Arlot, J.-E., 1996, *A&A* 314, 312
Bigourdan, G.: 1897, "Inventaire général et sommaire des manuscrits de la bibliothèque de l'observatoire Paris" *Ann. Obs. Pans* 21, F1-F60. [Delisle manuscripts are filed under the heading Manuscripts A-5-1 through A-5-8]
Bigourdan, G., 1901, *A.-G. Pingré: Annales Célestes du dix-septième siècle*, Paris: Gauthier-Villars
Brouwer, D., 1952, *AJ* 57, 126
Campbell, J. K., Synnott, S. P., 1985, *AJ* 90, 364
Davies, M. E., Abalakin, V. K., Bursa, M., Lederle, T., Lieske, J. H., Rapp, R. H., Seidelmann, P. K., Sinclair, A. T., Teifel, V. G., Tjuflin, Y. S.: 1986, *Celest. Mech.* 39, 103
Descamps, P., 1994, *A&A* 291, 664
Franklin, F., et al. ["Galilean Satellite Observers"], 1991, *AJ* 102, 806
Franklin, F., 1993, Personal communication
Gaskell, R. W.: 1995, Personal Communication
Goguen, J. D., Sinton, W. M., Matson, D. L., Howell, R. R., Dyck, H. M., Johnson, T. V., Brown, R. H., Veeder, G. J., Lane, A. L., Nelson, R. M., McLaren, R. A., 1988, *Icarus* 76, 465
Goguen, J. D.: 1994, Personal Communication
Kaas, A. A., Franklin, F., Aksnes, K., Lieske, J. H., 1997, "Mutual phenomena of the Galilean satellites 1990-1991", *AJ* [in press]
Lieske, J. H., 1977, *A&A* 56, 333 [referred to as *Theory*]
Lieske, J. H., Lederle, T., Fricke, W., Morando, B., 1977, *A&A* 58, 1
Lieske, J. H., 1979, *A&A* 73, 28

Table 7. Series coefficients for ephemerides E5

[Actual height is about 26.5 cm and covers 2 pages]

Table 7. Series Coefficients for E5

Index	E5	Argument	Ratio n/n_{ref}
XI-1 Series coefficients for $\xi_1 = (p_1 - a_1)/a_1$ (cosine)			
1	171	$t_1 - t_2$	50181707
2	100	$t_1 - t_2$	75272560
3	-2	$t_1 - t_2$	90028001
4	-1	$t_1 - t_2$	9006774
5	-187	$t_1 - t_2$	9006774
6	-214	$t_1 - t_2$	9006774
7	-66	$t_1 + \pi_1 - 2\pi_j - 2G$	90021435
8	-11339	$2t_1 - 2t_2$	103634113
9	3	$2t_1 - 2t_2$	150545120
10	-131	$4t_1 - 4t_2$	200726827
V-1 Series coefficients for $v_1 = v_1 - t_1$ (sine)			
1	-26	$-2\pi_j + 2v - 2G$	-00001870
2	-553	$-2\pi_j + 2v$	-00000072
3	-240	$-2\pi_j + \omega_1 + v - 2G$	-00005196
4	92	$-\omega_1 + v$	00010603
5	-74	$-\omega_1 + v$	00013528
6	-40	$-\omega_1 + v$	00010664
7	-425	G	00040634
8	65	$2G$	00016668
9	-33	$5G^2 - 2G + \phi_1$	00000647
10	-27	$\omega_1 - \omega_4$	-00002662
11	145	$\omega_2 - \omega_3$	-00012509
12	30	$\omega_2 - \omega_3$	-00015171
13	-U	$\pi_4 - \pi_1$	00006004
14	-6071	$t_1 - \pi_4$	00002598
15	262	$\pi_2 - \pi_1$	00016774
16	156	$\pi_2 - \pi_1$	00022322
17	-38	$\pi_1 - \pi_4$	00075407
18	-27	$\pi_1 - \pi_4$	00075405
19	-27	$\pi_1 + \pi_4 - 2\pi_j - 2G$	-00001454
20	-1176	$\pi_1 + \pi_4 - 2\pi_j - 2G$	00001144
21	1268	ϕ_1	00085406
22	39	$3t_2 - 7t_4 + 4\pi_4$	-00018335
23	-32	$3t_2 - 7t_4 + \pi_3 + 3\pi_4$	-00015737
24	-1162	$t_1 - 2t_2 + \pi_4$	00064318
25	-1887	$t_1 - 2t_2 + \pi_4$	00066016
26	-1244	$t_1 - 2t_2 + \pi_4$	00038640
27	33	$t_1 - 2t_2 + \pi_1$	00442723
28	-617	$t_1 - t_2$	50181707
29	-270	$t_1 - t_2$	75272560
30	-26	$t_1 - t_2$	89399390
31	4	$t_1 - \pi_1$	90020691
32	5	$t_1 - \pi_2$	90076774
33	776	$t_1 - \pi_3$	90066497
34	149	$t_1 - \pi_4$	90066506
35	21	$t_1 + \pi_4 - 2\pi_j - 2G$	90031633
36	-200	$2t_1 - 4t_2 + \omega_2 + \omega_3$	00070764
37	82483	$2t_1 - 4t_2 + 2\omega_2$	00694756
38	-35	$2t_1 - 2t_2$	100363413
39	-3	$2t_1 - 2t_2$	150645120
40	-3	$3t_1 - 4t_2 + \pi_3$	10073030
41		$4t_1 - 4t_2$	200726827

i

Table 7. Series Coefficients for E5, Continued

Index	E5	Argument	Ratio n/n_{ref}
LAT-1 Series coefficients for $\xi_1 = (p_1 - a_1)/a_1$ (sine)			
1	46	$t_1 - 2\pi_j + v - 2G$	90018331
2	6301	$t_1 - \omega_1$	100063250
3	1825	$t_1 - \omega_2$	100010136
4	120	$t_1 - \omega_3$	100003527
5	183	$t_1 - \omega_4$	100000665
6	-311	$t_1 - v$	100000001
7	75	$t_1 - 4t_2 + \omega_2$	100710791
XI-2 Series coefficients for $\xi_2 = (p_2 - a_2)/a_2$ (cosine)			
1		$2t_2 - \omega_1$	-00025108
2	-17	$2t_2 - 2\pi_j - 2G$	90106590
3	333	$t_2 - t_1$	50364739
4	45	$t_2 - t_1$	74721450
5	-102	$t_2 - \pi_1$	90040603
6	-1442	$t_2 - 2$	90053374
7	-3116	$t_2 - 2$	90092069
8	-1744	$t_2 - \pi_1$	90091145
9	-15	$2t_2 - \pi_j - G$	90114034
10	-w	$2t_2 - 2\omega_1$	157442901
11	164	$2t_2 - 2\omega_2$	20064376
12	18	$2t_2 - \omega_2 - \omega_3$	200039268
13	-U	$3t_2 - 3t_1$	2.3182685
14	-33	$t_1 - 2t_2 + \pi_1$	00731293
15	-67	$t_1 - 2t_2 + \pi_1$	00736509
16	9048	$t_1 - t_2$	100729474
17	48	$t_1 - 2t_2 + \pi_4$	10140771
18	107	$t_1 - 2t_2 + \pi_1$	10145987
19	-19	$t_1 - 2t_2 + \pi_2$	101505578
20	523	$t_1 - t_2$	151094217
21	30	$t_1 - \pi_1$	20722447
22	-290	$2t_1 - 2t_2$	201458956
23	-91	$2t_1 - 2t_2$	20218434
24	22	$4t_1 - 4t_2$	402917912
V-2 Series coefficients for $v_2 = t_2 - t_1$ (sine)			
1	98	$-2\pi_j + 2v - 2G$	-00163936
2	-1353	$-2\pi_j + 2v$	-00000004
3	331	$-2\pi_j + \omega_1 + v - 2G$	-00171013
4	38	$-2\pi_j + \omega_2 + v - 2G$	-00106122
5	31	$-\omega_2 + v$	-00032186
6	265	$-\omega_2 + v$	-00007078
7	218	$-\omega_2 + v$	-00001733
8	-1845	G	00081966
9	-253	$2G$	-00163932
10	18	$2G^2 - 2G + \phi_1$	-00007920
11	19	$2G^2 - G + \phi_1$	-00013954
12	-15	$3G^2 - 3G + \phi_1$	-00008067
13	-130	$3G^2 - 3G + \phi_1$	-00001098
14	102	$\omega_2 - \omega_1$	-00006344
15	36	$\omega_2 - \omega_1$	-00025108
16	72	$\omega_2 - \omega_1$	-00001815
17	2250	$\pi_1 - \pi_4$	00005216
18	-24	$\pi_1 - \pi_4 + \omega_2 - \omega_1$	-00000129
19	-23	$\pi_2 - \pi_1$	-00039591
20	-36	$\pi_2 - \pi_1$	-00044807
21	-31	$\pi_1 - 2$	00112575

ii

Table 7. Series Coefficients for E5, Continued

Index	E5	Argument	Ratio n/n_{ref}
XI-3 Series coefficients for $\xi_3 = (p_3 - a_3)/a_3$ (cosine)			
22	4	$\pi_1 - \pi_2$	00152167
23	111	$\pi_1 - \pi_4$	00157382
24		$\pi_1 + \pi_2 - 2\pi_j - 2G$	00002206
25	-3102	ϕ_1	00171435
26	55	$2t_3 - 2\pi_j - 2G$	90106590
27	-111	$3t_1 - 7t_4 + 4\pi_4$	-00036805
28	91	$3t_1 - 7t_4 + \pi_3 + 3\pi_4$	-00031589
29	-25	$3t_1 - 7t_4 + \pi_3 + 3\pi_4$	-00026373
30	-1994	$t_2 - t_1$	50364739
31	-137	$t_2 - t_1$	74721450
32	1	$t_2 - \pi_1$	90040803
33	2846	$t_2 - \pi_2$	90053378
34	6250	$t_2 - \pi_3$	90092069
35	3463	$t_2 - \pi_4$	90094185
36	30	$t_2 - \pi_j - C$	90018034
37	-18	$2t_2 - 3t_1 + \pi_4$	51000332
38	-39	$2t_2 - 3t_1 + \pi_4$	51101348
39	98	$2t_2 - 2t_1$	13744237
40	-164	$2t_2 - 2t_2$	200064376
41	-18	$2t_2 - \omega_2 - \omega_3$	200039268
42	72	$3t_1 - 5t_2$	351823695
43	30	$t_1 - 2t_2 - \pi_1 + 2\pi_j + 2G$	00068379
44	4180	$t_1 - 2t_2 + \pi_4$	00731293
45	747	$t_1 - 2t_2 + \pi_1$	00736509
46	-219	$t_1 - 2t_2 + \pi_2$	00776100
47	-19	$t_1 - 2t_2 + \pi_1$	00066575
48	-18505	$t_1 - t_2$	100729474
49	-110	$t_1 - 2t_2 + \pi_4$	101460771
50	-200	$t_1 - 2t_2 + \pi_1$	101463987
51	39	$t_1 - 2t_2 + \pi_2$	101505578
52	-16	$t_1 - 2t_2 + \pi_1$	10161453
53	-803	$t_1 - t_1$	151064217
54	-19	$t_1 - t_1$	200064376
55	-75	$t_1 - \pi_1$	200722447
56	-11	$t_1 - \pi_1$	200727663
57	-9	$2t_1 - 4t_2 + \omega_2 + v$	01451874
58	4	$2t_1 - 4t_2 + \omega_2 + v$	01444797
59	-14	$2t_1 - 4t_2 + \omega_2 + v$	01419688
60	150	$2t_1 - 4t_2 + \omega_2 + v$	01394580
61	-11	$2t_1 - 2t_2 - 2\pi_j - 2G$	01622868
62	-9	$2t_1 - 4t_2 + \pi_1 + \pi_2$	01607472
63	-8	$2t_1 - 4t_2 + \pi_1 + \pi_2$	01473017
64	915	$2t_1 - 2t_2 + 2\pi_1$	201358056
65	96	$2t_1 - 2t_2$	302184434
66	-18	$4t_1 - 4t_2$	402917912
LAT-2 Series coefficients for $\xi_2 = 2t_2/a_2$ (sine)			
1	17	$t_2 - 2\pi_j + v - 2G$	90754101
2	141	$t_2 - 2\pi_j + v - 2G$	90030868
3	-114	$t_2 - \omega_1$	100100001
4	81001	$t_2 - \omega_2$	100142188
5	1512	$t_2 - \omega_3$	100017980
6	1160	$t_2 - \omega_4$	100017135
7	-19	$t_2 - v$	90018036
8	-1284	$t_2 - v$	100000072
9	15	$t_2 - v + G$	100001068
10	-28	$t_2 - 2t_1 + \omega_1$	101451876
11	272	$t_2 - 2t_1 + \omega_1$	101126766

iii

Table 7. Series Coefficients for E-5, Continued

Index	E5	Argument	Ratio n/n_{ref}
XI-3 Series coefficients for $\xi_3 = (p_3 - a_3)/a_3$ (cosine)			
1	24	$-\omega_3 + v$	00014250
2	-9	$-\omega_3 - \omega_4$	-00010767
3	10	$\pi_3 - \pi_4$	00010508
4	294	$t_3 - t_1$	57130175
5	18	$t_3 - 2$	90006071
6	-14388	$t_3 - \pi_1$	90045835
7	-7919	$t_3 - \pi_2$	90096343
8	-23	$t_3 - \pi_j - G$	90045844
9	-20	$t_3 + \pi_4 - 2\pi_j - 2G$	90073384
10	-51	$t_3 + \pi_4 - 2\pi_j - 2G$	90068392
11	39	$2t_3 - 3t_1 + \pi_1$	71394181
12	-1761	$3t_3 - 2t_1$	114280349
13	-21	$3t_3 - 2\pi_1$	100971671
14	-10	$2t_3 - \pi_1 - \pi_4$	100042179
15	-27	$2t_3 - \pi_1 - 2G$	100069728
16	24	$2t_3 - 2\omega_1$	200028527
17	9	$2t_3 - \omega_2 - \omega_3$	200017760
18	-24	$2t_3 - \pi_1 - \pi_4$	200014268
19	-16	$t_3 - 4t_2 + \pi_1$	125324355
20	-156	$3t_1 - 3t_2$	171308524
21	-42	$3t_1 - 4t_2$	226520699
22	-11	$3t_1 - 5t_2$	285650873
23	6342	$t_3 - t_1$	101460677
24	9	$t_3 - \pi_1$	201455512
25	39	$t_3 - 2t_1 + \pi_1$	102583011
26	70	$t_3 - 2t_1 + \pi_1$	102953519
27	10	$t_1 - 2t_2 + \pi_1$	10143334
28	20	$t_1 - 2t_2 + \pi_1$	01483842
29	-153	$t_1 - t_2$	202939354
30	156	$t_1 - t_2$	304400031
31	11	$2t_1 - 2t_2$	405876708
V-3 Series coefficients for $v_3 = v_3 - t_3$ (sine)			
1	10	$-\pi_3 + \pi_4 - \omega_3 + v$	-00003751
2	28	$-2\pi_j + 2v - 2G$	-000382281
3	-1770	$-2\pi_j + 2v$	-00000000
4	-48	$-2\pi_j + \omega_1 + v - 2G$	-000144540
5	14	$-\omega_3 + v$	-00064845
6	111	$-\omega_3 + v$	-00014250
7	345	$-\omega_3 + v$	-00014492
8	-1338	G	00165146
9	-86	$2G$	00038222
10	10	$2G^2 - G + \phi_1$	-00009610
11	22	$2G^2 - 2G + \phi_1$	-00107274
12	28	$2G^2 - G + \phi_1$	-00032112
13	11	$2G^2 - 2G + \phi_1$	-00107471
14	9	$2G^2 - G + \phi_1$	-00014355
15	-19	$2G^2 - 3G + \phi_1$	-00162023
16	-208	$2G^2 - 2G + \phi_1$	-00017211
17	150	$\omega_3 - \omega_1$	-00010767
18	21	$\omega_3 - \omega_1$	-00045846
19	19	$\omega_3 - \pi_1$	-00000000
20	6034	$\pi_3 - \pi_4$	-00010508
21	-65	$\pi_3 - \pi_4 + \omega_3 - \omega_1$	-00007250
22	-98	$\pi_3 - \pi_4$	-00007078
23	-1	$\pi_3 - \pi_4$	-00002771
24	-98	$\pi_1 - \pi_4$	-00005791

iv

Table 7. Series Coefficients for E5, Continued

Index	E5	Argument	Ratio n/n_{sat}
25	-9	$\pi_1 - \pi_2$	0.00317978
26	-10	$\pi_1 - \pi_2 - 2\pi_1 - 2\pi_2$	0.00015041
27	-125	$\pi_1 - \pi_2 - 2\pi_1 - 2\pi_2$	0.0004827
28	107	π_1	0.00145300
29	-10	π_1	0.0006169
30	-111	$\pi_1 - 2\pi_1 + \pi_2$	0.0006086
31	-93	$\pi_1 - 2\pi_1 + \pi_2$	0.0006114
32	-94	$\pi_1 - \pi_2$	0.0006175
33	-17	$\pi_1 - \pi_2$	0.0006071
34	28740	$\pi_1 - \pi_2$	0.0005435
35	1.10	$\pi_1 - \pi_2$	0.0006113
36	7	$\pi_1 - \pi_2 + \omega_1 - \omega_2$	0.0005576
37	16	$\pi_1 - \pi_2 - G$	0.00034664
38	51	$\pi_1 - \pi_2 - 2G$	0.00073344
39	11	$\pi_1 + \pi_2 - 2\pi_1 - 3G$	0.0008756
40	97	$\pi_1 + \pi_2 - 2\pi_1 - 2G$	0.00083402
41	11	$2\pi_1 - 3\pi_2 + \pi_3$	0.0006162
42	-101	$2\pi_1 - 3\pi_2 + \pi_3$	0.0006181
43	1.3	$2\pi_1 - 3\pi_2 + \pi_3$	0.0006189
44	3222	$2\pi_1 - 2\pi_2$	0.00060340
45	29	$2\pi_1 - 2\pi_2$	0.00071871
46	25	$2\pi_1 - \pi_2$	0.00082179
47	37	$2\pi_1 - 2\pi_1 - 2G$	0.00089728
48	-24	$2\pi_1 - 348$	0.00082527
49	-0	$2\pi_1 - \omega_2 - \omega_4$	0.00017760
50	24	$2\pi_1 - \omega_2 - \omega_4$	0.00014268
51	-174	$3\pi_1 - 7\pi_2 + 3\pi_3$	0.00074150
52	140	$3\pi_1 - 7\pi_2 + 3\pi_3 + 3\pi_4$	0.00083642
53	-55	$3\pi_1 - 7\pi_2 + 2\pi_3 + 2\pi_4$	0.00083134
54	27	$3\pi_1 - 4\pi_2 + \pi_3$	0.00084355
55	227	$3\pi_1 - 3\pi_2$	0.00080524
56	53	$4\pi_1 - 4\pi_2$	0.00080690
57	13	$5\pi_1 - 5\pi_2$	0.00080673
58	42	$\pi_1 - 3\pi_1 + 2\pi_2$	0.00093672
59	-12855	$\pi_1 - \pi_2$	0.00086677
60	-24	$\pi_1 - \pi_2$	0.00083312
61	-10	$\pi_1 - \pi_2$	0.0008020
62	-79	$2\pi_1 - 3\pi_2 + \pi_3$	0.00082011
63	-131	$2\pi_1 - 3\pi_2 + \pi_3$	0.00083519
64	-665	$\pi_1 - 2\pi_1 + \pi_2$	0.00083334
65	-1226	$\pi_1 - 2\pi_1 + \pi_2$	0.00082642
66	1082	$\pi_1 - 2\pi_1 + \pi_2$	0.00083806
67	m	$\pi_1 - 2\pi_1 + \pi_2$	0.00082111
68	192	$\pi_1 - \pi_2$	0.00082200
69	218	$2\pi_1 - 4\pi_2 + \omega_3 + \omega_4$	0.00080331
70	2	$2\pi_1 - 4\pi_2 + \omega_3$	0.0008086
71	-4	$2\pi_1 - 4\pi_2 + 2\omega_3$	0.00080877
72	3	$2\pi_1 - 4\pi_2 + 2\omega_3$	0.00080655
73	2	$2\pi_1 - 4\pi_2 + \pi_3 + \pi_4$	0.00081715
74	2	$2\pi_1 - 4\pi_2 + 2\pi_3$	0.00081683
75	-13	$2\pi_1 - 2\pi_1$	0.00087808

LAT-3: Series coefficients for $\zeta_3 = \pi_3/\pi_2$ (sine)

1	37	$\zeta_3 - 2\pi_1 + \pi_2 - 3G$	0.0004587
2	371	$\zeta_3 - 2\pi_1 + \pi_2 - 2G$	0.00069734
3	-15	$\zeta_3 - 2\pi_1 + \pi_2 - G$	0.0004860
4	-45	$\zeta_3 - 2\pi_1 + \pi_2$	0.0009096
5	-2797	$\zeta_3 - \omega_2$	0.00064819

V

Table 7. Series Coefficients for E5, Continued

Index	E5	Argument	Ratio n/n_{sat}
4	12872	$\pi_1 - \pi_2$	0.00014263
7	9447	$\pi_1 - \pi_2$	0.0003406
9	-45	$\pi_1 - \pi_2 - G$	0.00034664
4	-16011	$\pi_1 - \pi_2$	0.00030000
10	51	$\pi_1 - \pi_2 + G$	0.00065140
11	10	$2\pi_1 - 3\pi_2 + \omega_3$	0.00030350
12	-21	$2\pi_1 - 3\pi_2 + \omega_3$	0.00030350
13	30	$2\pi_1 - 3\pi_2 + \omega_3$	0.00034505

--- LAT-4: Series coefficients for $\zeta_4 = \pi_4/\pi_2$ (cosine)

1	-19	$-\omega_1 + \omega_2$	0.00032262
2	167	$-\omega_1 + \omega_2$	0.0008146
3	11	G	0.00034064
4	12	$\pi_1 - \pi_2$	0.00024511
5	-13	$\pi_1 - \pi_2$	0.0006059
6	1611	$\pi_1 - \pi_2$	0.0001451
7	-24	$\pi_1 - \pi_2 - 2\pi_1 + 2\omega_2$	0.0006268
8	-17	$\pi_1 - \pi_2 - G$	0.0001470
9	-73546	$\pi_1 - \pi_2$	0.00076674
10	15	$\pi_1 - \pi_2 + G$	0.0001489
11	30	$\pi_1 - \pi_2 + 2\pi_1 - 2\omega_2$	0.0002953
12	-5	$\pi_1 - \pi_2 - 2G$	0.00014796
13	-89	$\pi_1 - \pi_2 - G$	0.00000000
14	182	$\pi_1 - \pi_2$	0.00067715
15	-6	$\pi_1 + \pi_2 - 2\pi_1 - 4G$	0.00052919
16	-62	$\pi_1 + \pi_2 - 2\pi_1 - 3G$	0.00038122
17	-543	$\pi_1 + \pi_2 - 2\pi_1 - 2G$	0.00023326
18	27	$\pi_1 + \pi_2 - 2\pi_1 - G$	0.00006530
19	6	$\pi_1 + \pi_2 - 2\pi_1$	0.00016696
20	6	$\pi_1 + \pi_2 - \omega_1 - \omega_2$	0.00015981
21	-9	$\pi_1 + \pi_2 - 2\pi_1 - 2G$	0.00036334
22	14	$2\pi_1 - \pi_1$	0.00054329
23	13	$2\pi_1 - \pi_1$	0.00082940
24	-271	$2\pi_1 - 2\pi_1 - 3G$	0.00044389
25	-25	$2\pi_1 - 2\pi_1 - 2G$	0.00029593
26	-155	$2\pi_1 - 2\pi_1 - \omega_1$	0.00041428
27	-12	$2\pi_1 - \omega_2 - \omega_4$	0.00033281
28	19	$2\pi_1 - \omega_2 - \omega_4$	0.00033281
29	-48	$2\pi_1 - 2\pi_1$	0.0006312
30	-167	$2\pi_1 - 2\pi_1 - \omega_1$	0.0008168
31	142	$2\pi_1 - 2\pi_1$	0.00000019
32	-22	$\pi_1 - 2\pi_1 + \pi_2$	0.00072835
33	20	$\pi_1 - 2\pi_1 + \pi_2$	0.00072835
34	974	$\pi_1 - \pi_2$	0.00064306
35	24	$2\pi_1 - 2\pi_1 + \pi_2$	0.00027129
36	177	$2\pi_1 - 2\pi_1$	0.00022409
37	4	$3\pi_1 - 4\pi_2 + \pi_3$	0.00001444
38	42	$3\pi_1 - 2\pi_1$	0.0002914
39	14	$4\pi_1 - 4\pi_2$	0.00057219
40	8	$3\pi_1 - 3\pi_2$	0.00022574
41	-8	$\pi_1 - 3\pi_2 + 2\pi_1$	0.00036073
42	92	$\pi_1 - \pi_1$	0.0005841
43	106	$\pi_1 - \pi_1$	0.00041914

VI

Table 7. Series Coefficients for E5, Continued

Index	E5	Argument	Ratio n/n_{sat}
--- LAT-3: Series coefficients for $\zeta_3 = \pi_3/\pi_2$ (sine) ---			
1	8	$-\pi_1 - \pi_2 + 2\omega_2$	0.00041590
2	-9	$-\pi_1 - \pi_2 + \omega_1 + \omega_2$	0.00049737
3	27	$-\pi_1 - \pi_2 + \omega_1 + \omega_2$	0.00016365
4	-409	$-2\pi_1 + 2\omega_2$	0.00017079
5	310	$-2\pi_1 + \omega_1 + \omega_2$	0.00025226
6	-19	$-2\pi_1 + \omega_1 + \omega_2$	0.00050341
7	8	$-\pi_1 - \pi_1 + 2\omega_2$	0.00068549
8	-5	$-\pi_1 - \pi_1 + \omega_1 + \omega_2$	0.00016696
9	63	$-\pi_1 + \pi_1 - \omega_1 + \omega_2$	0.0000384
10	8	$-2\pi_1 + 2\omega_2 - 3G$	0.00015630
11	73	$-2\pi_1 + 2\omega_2 - 2G$	0.00070427
12	-3768	$-2\pi_1 + 2\omega_2$	0.00000019
13	16	$-2\pi_1 + \omega_1 + \omega_2 - 2G$	0.00074573
14	-97	$-\omega_1 + \omega_2$	0.0003262
15	152	$-2\omega_1 + 2\omega_2$	0.00016293
16	3070	$-\omega_1 + \omega_2$	0.0008146
17	-5604	G	0.00035204
18	-204	$2G$	0.00070407
19	-10	$3G$	0.00015611
20	24	$G^2 - G + \omega_2$	0.00030090
21	11	$G^2 + \omega_1 - 2\omega_2$	0.00015514
22	52	$2G^2 - 2G + \omega_1$	0.00080140
23	61	$2G^2 - G + \omega_1$	0.00074976
24	25	$3G^2 - 2G + \omega_1 + \omega_2$	0.00030566
25	21	$3G^2 - G + \omega_1 - \omega_2$	0.0000138
26	-45	$5G^2 - 3G + \omega_1$	0.00040042
27	-105	$5G^2 - 2G + \omega_2$	0.0005162
28	-44	$-\omega_1 - \omega_2$	0.00025116
29	5	$\pi_1 - \pi_1 - G^2$	0.00076674
30	234	$\pi_1 - \pi_1$	0.00006530
31	11	$2\pi_1 - 2\pi_1 - 2G$	0.00073348
32	-10	$2\pi_1 - \omega_2 - \omega_4$	0.00084487
33	68	$2\pi_1 - 2\omega_2$	0.00033372
34	-13	$\pi_1 - \pi_1 - \omega_1 + \omega_2$	0.00032658
35	-5068	$\pi_1 - \pi_1$	0.00024511
36	-47	$\pi_1 - \pi_1$	0.00081694
37	-1219	$\pi_1 - \pi_1$	0.0006059
38	48	$\pi_1 - \pi_1 - 2\pi_1 + 2\omega_2$	0.0001451
39	10	$\pi_1 - \pi_1 - \omega_1 + \omega_2$	0.00006110
40	53	$\pi_1 - \pi_1 - G$	0.00086268
41	117108	$\pi_1 - \pi_1$	0.0001170
42	-11	$\pi_1 - \pi_1 + G$	0.00076674
43	-11	$\pi_1 - \pi_1 + \omega_1 - \omega_2$	0.00081324
44	-61	$\pi_1 - \pi_1 - 2\pi_1 - 2\omega_2$	0.00011809
45	10	$\pi_1 - \pi_1 - G$	0.00022503
46	174	$\pi_1 - \pi_1 - G$	0.00014796
47	-11.1	$\pi_1 - \pi_1$	0.00000000
48	5	$\pi_1 + \pi_1 - 2\pi_1 - 3G^2 + 2G - \omega_1$	0.00003368
49	1.2	$\pi_1 + \pi_1 - 2\pi_1 - 4G^2$	0.00067715
50	124	$\pi_1 + \pi_1 - 2\pi_1 - 3G^2$	0.00052919
51	1088	$\pi_1 + \pi_1 - 2\pi_1 - 2G^2$	0.00034122
52	-55	$\pi_1 + \pi_1 - 2\pi_1 - G$	0.00021326
53	-12	$\pi_1 + \pi_1 - 2\pi_1$	0.00006530
54	-14	$\pi_1 + \pi_1 - \omega_1 - \omega_2$	0.00014006
55	6	$\pi_1 + \pi_1 - 2\pi_1$	0.00006549
56	17	$\pi_1 + \pi_1 - 2\pi_1$	0.00015981
57	-28	$\pi_1 + \pi_1 - 2\pi_1 - 2G$	0.00026631

VII

Table 7. Series Coefficients for E5, Continued

Index	E5	Argument	Ratio n/n_{sat}
58	-33	$2\ell_1 - \pi_3$	1.99958429
59	676	$2\ell_1 - 2\pi_4$	1.99982940
60	36	$2\ell_1 - 2\pi_1 - 3G$	1.98444389
61	218	$2\ell_1 - 2\pi_1 - 2G$	1.9922953
62	-5	$2\ell_1 - 2\pi_1 - G$	1.99614796
63	-1	$2\ell_1 - 4\pi_3 - \omega_4$? 00041428
64	-19	$2(\ell_1 - 4\pi_3 - V)$	2.00033281
65	-48	$2\ell_1 - \pi_2$	2.00016312
66	167	$2\ell_1 - \omega_1 - \nu$	2.00008166
67	-142	$2\ell_1 - 2\nu$	2.00000019
68	148	$\ell_1 - 2\ell_1 + \pi_1$	0.00027835
69	-94	$(\ell_1 - 2\ell_1 + \pi_1)$	22.27346
70	-300	$G - \ell_1$	1.33264305
71	9	$2\ell_1 - 4\ell_1 + 2\pi_1$	665.45660
72	-37	$2\ell_1 - 3\ell_1 + \pi_1$? 66537139
73	6	$2\ell_1 - 3\ell_1 + \pi_1$	1.66561651
74	-195	$3\ell_1 - 7(\ell_1 + 2\pi_1 + \omega_1 + \nu)$	2.66526690
75	6	$3\ell_1 - 7\ell_1 + 4\pi_1$	- 0.0138192
76	187	$3\ell_1 - 7\ell_1 + 4\pi_1$	- 0.0172966
77	-149	$3\ell_1 - 7\ell_1 + 2\pi_1 + 3\pi_2$	- 0.0148455
78	51	$3\ell_1 - 7\ell_1 + 2\pi_1 + 3\pi_2$	- 0.0123943
79	-10	$3\ell_1 - 7\ell_1 + 3\pi_1 + \pi_1$	- 0.0099432
80	6	$3\ell_1 - 6\ell_1 + 3\pi_1$	998.04504
81	-8	$3\ell_1 - 4\ell_1 + \pi_1$? 99801444
82	-41	$3\ell_1 - 3\ell_1$	1.99792914
83	-13	$4\ell_1 - 4\ell_1$	5.33057219
84	-44	$\ell_1 - 3\ell_1 + 2\ell_1$	- 29836073
85	89	$\ell_1 - \ell_1$	3.6905841
86	106	$\ell_1 - \ell_1$	8.43341914

--- LAT-4: Series coefficients for $\zeta_4 = \pi_4/\pi_2$ (sine) ---

1	8	$\ell_1 - 2\pi_1 - \omega_1 + 2\nu$	1.00006137
2	4	$\ell_1 - 2\pi_1 - \omega_1 - 4G$	0.00450175
3	48	$\ell_1 - 2\pi_1 + \omega_1 - 3G$	9.98444379
4	773	$\ell_1 - 2\pi_1 + \omega_1 - 2G$	992.2953
5	-84	$\ell_1 - 2\pi_1 + \omega_1 - G$	9961.1747
6	5	$\ell_1 - 2\pi_1 + \nu$	99999990
7	9	$\ell_1 - \pi_1$	1.00015611
8	-17	$\ell_1 - \omega_1$	1.01151270
9	-511.2	$\ell_1 - \pi_1$	1.00013272
10	-7	$\ell_1 - \pi_1 - G$	99872252
11	141.34	$\ell_1 - \omega_1$	1.00000156
12	7	$\ell_1 - \pi_1 - G$	1.01193109
13	-102	$\ell_1 - \nu - G$	9981.49495
14	-765.79	$\ell_1 - \nu$	1.00000019
15	104	$\ell_1 - \nu + G$	1.01165213
16	-10	$\ell_1 - \nu + \omega_1 - 2G + \omega_2$	1.00005172
17	-11	$\ell_1 - 2\ell_1 + \nu$	13.2164295
18		$\ell_1 - 2\ell_1 + \omega_1$	132761.19

- Lieske, J.H., 1980, A&A 82, 340 [referred to as E2 ephemerides]
 Lieske, J.H., 1986a A&A 154, 61
 Lieske, J. H., 1986b A&AS 63, 143
 Lieske, J.H.H., 1987, A&A 176, 146
 Lieske, J.H., 1994a, "Galilean Satellite Ephemerides E4" JPL Engineering Memorandum 314-545 (19 June 1994) (JPL internal publication)
 Lieske, J. H., 1994b, A&A 281, 281
 Lieske, J. H., 1995, Bull. AAS 27, 1197
 Lindegren, L., 1977, A&A 57, 55
 Mallama, A., 1992a, Icarus 95, 309
 Mallama, A., 1992b, Icarus 97, 298
 Mallama, A., 1993, J. Geophys. Res. 98, p. 18.873-18.876
 Martin, C. F., 1969, Ph.D. Diss., Yale Univ.
 Monet, A. K. B., Stone, R. C., Monet, D. C., Dahn, C.C. Harris, H. C., Leggett, S. K., Pier, J. R., Vrba, F. J., Walker, R. L., 1994, AJ 107, 2290
 Monet, D. G., Monet, A. K. B., 1992, "Galilean satellite astrometry", U.S. Naval Observatory Flagstaff Station memorandum
 Monet, D. G., Dahn, C. C., Vrba, F. J., Harris, H. C., Pier, J. R., Luginbuhl, C. B., Ables, H. D., 1992, AJ 103, 638
 Morrison, L. V., Ward, C. G., 1975, MNRAS 173, 183
 Morrison, L. V., 1980, Personal Communication.
 Ostro, S. J., Campbell, D. B., Simpson, R. A., Hudson, R. S., Chandler, J. F., Rosema, K. D., Shapiro, I. I., Standish, E. M., WinJder, R., Yeomans, D. K., Velez, R., Goldstein, R. M., 1992, J. Geophys. Res. 97, p. 18.277
 Owen, W. M., 1993, Personal Communication
 Owen, W. M., 1995, Personal Communication
 Pascu, D., 1977, in: Planetary Satellites, ed. J.A. Burns, University of Arizona Press, Tucson, p. 63
 Pascu, D., 1979, in: Natural and Artificial Satellite Motion eds. P.E. Nacozy, S. Ferraz-Mello, University of Texas, Austin, p. 17
 Pascu, D., 1993, Personal Communication
 Pascu, D., 1994, in: Galactic and Solar System Optical Astrometry, eds. Morrison, L. V., Gilmore, G. F., Cambridge University Press, p. 304
 Pierce, D. A., 1980, "Observations of Jupiter's Satellites", JPL Engineering Memorandum 900-672.
 Pickering, E. C., 1907, Harvard Ann. 52, Part I, 1
 Riedel, J. E., 1994, Personal Communication
 Sampson, R. A., 1921, MRAS 63 [Sampson Theory]
 Spencer, J. 1993, Personal Communication
 Spencer Jones, H., 1939, MNRAS 99, 541
 Standish, E. M., 1982, A&A 114, 297
 Standish, E.M., 1985, "JPL Planetary Ephemerides DE125", JPL IOM 314.6-591
 Standish, E.M., Folkner, W.M., 1995, "JPL Ephemerides DE400 and DE I-10", JPL IOM 314.10-109
 Stephenson, F. R., Morrison, L. V., 1984, Phil. Trans. R. Soc. London, Ser. A, 313, 47
 Synnott, S. P., Donegan, A. J., Morabito, L. A., 1982, "Position Observations of the Galilean Satellites from Voyager Data", Jet Propulsion Laboratory internal document
 Vasundhara, R., 1994, A&A 281, 565
 West, R.M., 1992, in: Trans IAU XXIB, ed. J. Bergeron, Kluwer, Dordrecht, p. 211
 This article was processed by the author using Springer-Verlag L^AT_EX A&A style file LAA version 3.